Relative bioavailability assessment of solid forms by an artificial stomach and duodenum apparatus

Yiwang Guo, ¹ Alexander Byer-Alcorace ², Cody Thomas ², Stephanie Piekos, ² Laibin Luo, ³ Michael

Hawley, 3,4 Changquan Calvin Sun 1,*

¹Pharmaceutical Materials Science and Engineering Laboratory, Department of Pharmaceutics, College of

Pharmacy, University of Minnesota, 308 Harvard St. S.E. Minneapolis, MN 55455

² Drug Metabolism & Pharmacokinetics, Boehringer Ingelheim Pharmaceuticals Inc., 900 Ridgebury Road,

Ridgefield CT, 06877

^{3.} Material & Analytical Sciences, Boehringer Ingelheim Pharmaceuticals Inc., 900 Ridgebury Road,

Ridgefield, CT 06877

⁴ PharmSci Links, Stonington CT 06378 (current affiliation)

*Corresponding author

Changquan Calvin Sun, Ph.D.

9-127B Weaver-Densford Hall

308 Harvard Street S.E.

Minneapolis, MN 55455

Email: sunx0053@umn.edu

Tel: 612-624-3722

Fax: 612-626-212

1 Abstract

- 2 In this work, the ability of the artificial stomach and duodenum (ASD) model to predict bioavailability in rats was investigated using a poorly soluble model compound, BI-639667. A solution and four 3 4 suspensions of different solid forms of BI-639667 were tested both in an ASD and rats. Rank order of the 5 bioavailability estimated from ASD is consistent with that of *in vivo* result in rats, i.e., solution > salicylic acid cocrystal > malate salt > maleate salt > monohydrate. The results correlate with the ability of the 6 7 different solid forms to maintain supersaturation with respect to the stable form in aqueous solution. The 8 rank ordering of the results support the use of an ASD for characterizing dissolution performance of solid 9 forms to aid their selection for tablet formulation development.
- 10 Keywords
- 11 Biorelevant dissolution; artificial stomach and duodenum; cocrystal, salt, BI-639667

Introduction

12

13

14

15

16

17

18

19

20

21

22

23

24

25

26

27

28

29

30

31

32

33

34

35

36

It is highly efficient and economical for the development of an oral dosage form of a given active pharmaceutical ingredient (API) if relative in vivo bioavailability can be reliably predicted using an in vitro dissolution method (Wang et al., 2009). A key approach for developing a predictive in vitro dissolution method is to closely mimic in vivo conditions, such as fluid volume, secretion of gastric or intestinal fluids, fluid transport, pH change, and concentration of bio-salts, in the gastrointestinal (GI) tract (Fotaki and Vertzoni, 2010; Wang et al., 2009). Thus, the single compartment static systems commonly used in compendial methods, e.g., USP dissolution apparatuses I and II, although very valuable for quality control purposes and for biopharmaceutical classification system (BCS) class I APIs (high solubility and high permeability), are not reliable for predicting in vivo bioavailability of BCS class II APIs (low solubility and high permeability) exhibiting dissolution limited absorption. This is particularly critical for APIs that undergo complex phase change or pH sensitive precipitation behaviors in the dynamic GI tract (Carino et al., 2006; Guo and Sun, 2022). Thus, dissolution assessment performed with the USP apparatuses provides limited information to guide the selection of suitable solid forms for formulation development. Hence, systems that better mimic the GI tract have been developed for performing more predictive biorelevant dissolution tests (Takeuchi et al., 2014; Tsume et al., 2023; Tsume et al., 2015). Two main approaches of biorelevant dissolution are 1) the two-stage dissolution and 2) the transfer model. Since absorption takes place mainly in the intestine for most orally administered drugs, the knowledge of drug concentration – time profile in the intestine can reliably rank order the bioavailability of different formulations if the absorption is limited by dissolution not by permeation.

During two-stage dissolution, a formulation is initially put into gastric fluid and, after a certain time, simulated intestinal fluid is added to simulate the transfer of the gastric contents into intestine (Chen et al., 2022; Shah and Dong, 2022). Compared to the two-stage dissolution, a transfer model controls the kinetic of transferring both fluid and particles from a gastric chamber to an intestinal chamber (Kostewicz et al., 2004). This is advantageous because the fluid transfer kinetics can significantly affect drug dissolution and

precipitation (Kaur et al., 2020; Takeuchi et al., 2014; Vrbanac et al., 2020). This type of model is particularly useful for poorly soluble drugs exhibiting pH-dependent solubility in the physiological pH range. For example, weak bases can dissolve in the acidic gastric fluid but may precipitate out when mixed with the nearly neutral intestinal fluid, which can lead to low bioavailability (Guo and Sun, 2022; Kostewicz et al., 2004).

The earlier "transfer model" used a constant transferring rate from stomach to intestine (Kostewicz et al., 2004). More recently developed transfer models employed the first order stomach emptying process to more closely mimic the first order stomach emptying process in fasted state (Mudie et al., 2014). These include the advanced gastric simulator (Vrbanac et al., 2020), gastrointestinal simulator (Takeuchi et al., 2014), and artificial stomach and duodenum (ASD) (Carino et al., 2010). In addition, the use of biorelevant dissolution media can also provide more reliable predictions as precipitation kinetics of a drug in the small intestine may be affected by the presence of surfactant (e.g., bile salts) (Mithani, 1998; Mudie et al., 2020; Zhou et al., 2017; Zoeller and Klein, 2007).

Among these multi-compartment *in vitro* dissolution apparatuses, i.e., transfer dissolution model, the ASD is more suitable for routine formulation screening in the laboratory due to its low cost to assemble, repeatability, and simplicity, while adequately mimicking key *in vivo* physiological processes. The ASD simulates the upper parts of the GI tract, with two connected chambers representing stomach and duodenum. The gastric fluid is transferred to the duodenum chamber at a prescribed first-order rate to simulate the stomach emptying process. Meanwhile, fresh simulated gastric or intestinal fluid is introduced into the corresponding chamber to simulate the *in vivo* secretion of these fluids. The ability of the ASD to rank order relative bioavailability based on the AUC of drug in the duodenum chamber was shown using several BCS II drugs, e.g., different solid forms of carbamazepine in dogs (Carino et al., 2006), different formulations of LY2300559 in patients (Polster et al., 2015), and a model compound (Carino et al., 2010; P. Heinrich Stahl, 2002). Hence, ASD has been employed as a useful tool for solid forms screening, formulation

development, and understanding the effects of GI conditions on bioavailability (Carino et al., 2006; Carino et al., 2010; Lee et al., 2017; Polster et al., 2010; Polster et al., 2015; Tsume et al., 2015).

The purpose of this study was to further examine the reliability of ASD in predicting relative bioavailability of solid forms, including cocrystal and salt. A solution, a salicylic acid cocrystal, a maleate salt, a malate salt, and a hydrate of a BCS II compound, BI-639667 were evaluated both by ASD and rats. The *in vitro* and *in vivo* data were correlated to assess the predictability of *in vivo* bioavailability by the ASD.

Materials and Methods

Materials

BI-639667 (Figure 1, molecular weight: 451.5 g/mol) was kindly donated by Boehringer Ingelheim (Boehringer Ingelheim, CT) through Boehringer Ingelheim's opnMe molecule sharing program (opnMe.com, https://opnme.com/molecules/ccr1-bi639667). BI 639667 is a poorly water soluble basic compound with a pKa of 2.3 and an intrinsic solubility of about 5 μg/mL. In general, it has a strong propensity to precipitate when supersaturated. Salicylic acid, DL-malic acid were ACS reagent grade and maleic acid was HPLC grade (Sigma-Aldrich, St. Louis, MO). Acetonitrile and isopropanol were in ACS grade (Fisher Scientific, PA). Hydrochloric acid (36.5%-38%; VWR International, Eagan, MN), sodium phosphate monobasic monohydrate, and sodium phosphate dibasic heptahydrate (Fisher Scientific International, Inc., Fair Lawn, NJ) were used as received to prepare the *in vitro* dissolution medium.

Figure 1. Molecular structure of BI-639667 (MW of 451.5 g/mol)

Methods

Sample preparation

A 10 mg/mL solution of BI-639667 was prepared in a medium containing PEG 400 (55%, w/w), vitamin E TPGS (30%, w/w), ethanol (10%, w/w), and water (5%, w/w). A monohydrate form was obtained by suspending ~2 mmol (903 mg) API in 4 mL deionized water (DI water) for ~72 hr. All other crystal forms were prepared by suspending equal molar (2 mmol) of API and coformers in organic solvent (~3 mL acetonitrile for a salicylic acid cocrystal, ~3 mL isopropanol for a maleate acid salt, and ~15 mL acetonitrile for a malate salt) for ~72 hrs. The phase purity of various solid forms was checked by powder X-ray diffraction (PXRD) and differential scanning calorimetry (DSC).

Powder X-ray diffraction (PXRD)

PXRD patterns of the solid forms were obtained on a wide-angle X-ray diffraction instrument (X'Pert Pro; PANalytical Inc., West Borough, MA) using Cu K α radiation. The voltage and current applied were 45 kV and 40 mA, respectively. Each measurement was performed with a step size of 0.0167 $^{\circ}$ in the 2-theta range of 5-35 $^{\circ}$ and a dwell time of 1.15 s.

Intrinsic dissolution rate (IDR) study

IDR of BI solid forms was determined by the rotating disc method. The dissolution medium was pH 1.2 HCl solution. Approximately 20 mg of sample powder was compressed at a force of 1000 lb, using a custom-made stainless steel die, against a flat stainless steel disc for 2 min to prepare pellet (6.39 mm in diameter) with a visually smooth exposed surface that was coplanar with the surface of the die. While rotating at 300 rpm, the die was immersed in 200 mL of the dissolution medium at 37 °C, a UV-Vis fiberoptic probe (Ocean Optics, Dunedin, FL) was used to continuously monitor the UV absorbance of the medium. To avoid the spectra influence of other coformers, concentration of BI was determined at 350 nm (Figure S1).

Solubility measurement

pH-dependent solubility of BI-639667 was determined by adding excess BI-639667 powders into buffer solutions with a set of pHs (Table S1 and Figure S2) at room temperature. The solution concentration was determined by HPLC at both 24 hrs and 48 hrs to verify the equilibrium had been reached, solid forms were checked by PXRD.

Solubility of monohydrate form was determined by adding excessive monohydrate powders in DI water and being stirred for 96 hrs at room temperature, powder X-ray diffraction (PXRD) was utilized to confirm absence of phase transition. Concentration in solution was determined by UV spectrometry.

To measure apparent solubility of salicylic acid cocrystal, maleate salt, and malate salt in water at room temperature, HPMC 100K (0.1 and 1 mg/mL), HPMC AS-MF (0.1 mg/mL), PVP (0.1, 1 and 10 mg/mL), PVPVA (0.1, 1 and 10 mg/mL) were added in an effort to prevent or slow down their possible phase transition into less soluble forms (Table S2). This choice was based on the observation of fast phase transformation of maleate salt and malate salt to the monohydrate in an IDR study, where no phase change was detected for salicylic acid cocrystal (Figure S3). The suspensions were stirred in tightly capped vials, and the phase transition was monitored by identifying the isolated excess solid in each vial with PXRD. We only measured the solubility of salicylic acid cocrystal after 30 h (no phase transition detected) since maleate salt and malate salt were not sufficiently stable even with the presence of nucleation inhibitors in water.

In vitro ASD dissolution study

In vitro dissolution of each sample was determined using an artificial stomach duodenum (ASD) apparatus. The parameters were chosen based on typical physiological conditions in human fasted state (Dressman, 1986; Kararli, 1995) and previous ASD works (Polster et al., 2010; Wang et al., 2018). The ASD consists of two jacketed beakers with temperature controlled at 37 °C using a circulating water bath. It simulates both stomach and duodenum, where the fluid flow is regulated by a programmatically controlled peristaltic Masterflex L/S Easy-Load II pump (Cole-Parmer, Vernon Hills, IL).

Experiments were conducted with 0.01 N HCl (pH = 2) for the stomach and 0.1 M sodium phosphate buffer (pH = 6.8) for the duodenum. The initial volume of the stomach chamber was 250 mL, which was decreased to 50 mL by first-order emptying with a half-life of 15 min. The duodenum volume was maintained at 30 mL throughout the entire study, achieved by setting a vacuum line in the duodenum chamber at a calibrated height. In addition, the chambers were infused with fresh gastric or duodenal liquid at 2 mL/min to mimic *in vivo* secretion processes. Drug concentration was determined from the absorbance signals obtained by a fiber optic UV/vis probe. Mixing was achieved by an overhead paddle stirrer in the stomach chamber and a magnetic stirrer in the duodenum chamber. Prior to each experiment, calibration of all pumps and spectrometers were performed. All fluids used in the experiment were degassed to avoid the generation of bubbles during the course of the experiment that might interfere the real-time concentration monitoring by UV/vis probe.

The drug concentration—time profile in the duodenum was analyzed by PKsolver 2.0, and the noncompartmental method was used to calculate key pharmacokinetic parameters, including peak plasma concentration (C_{max}), time to reach C_{max} (T_{max}), and area under the plasma concentration—time curve (AUC).

Evaluation of BI-639667 pharmacokinetics in rats

Animal preparation

Male Wistar Han rats (n=20) weighing approximately 250 g were fitted with jugular vein catheters and vascular access buttons (Instech Laboratories, Plymouth Meeting, PA) by the vendor (Charles River Laboratories, Wilmington, MA). Prior to compound administration, rats were fasted overnight with water provided *ad libitum*, and food was returned 4 h after dosing. Animal care and study procedures were approved by the Institutional Animal Care and Use Committee of Boehringer Ingelheim Pharmaceuticals, Inc. (Ridgefield, CT) and were performed in accordance with the NIH's *Guide for the Care and Use of Laboratory Animals*.

Compound administration

Rats were randomly divided into five groups of four, and each group was administered one of the five formulations (50 mg/kg equivalent dose of BI-639667), i.e., solution, monohydrate solid, salicylic acid cocrystal solid, malate salt, and maleate salt, via oral gavage under isoflurane anesthesia. To dose the solid powders, disposable gavage tubes (13-15 G) were coated with magnesium stearate to prevent particle adherence, and a plunger was placed to push the solid through the tubes. Each administered formulation, except for the solution, was followed by a flush of saline administered orally via gavage. Rats were allowed to recover from anesthesia before blood collections were initiated.

Blood sampling and preparation of plasma for bioanalysis

Blood samples were collected from each animal via a jugular vein catheter at 0.25, 0.5, 1, 2, 4, 6, 8, 24, and 48 h after dosing and placed into tubes containing K₃-EDTA as an anticoagulant. Samples were kept on ice then centrifuged at 10,000 g for 5 min at 4 °C to collect plasma, and plasma samples were then stored at -80 °C prior to bioanalysis. Plasma protein was precipitated by adding acetonitrile, which contained 1% acetic acid and verapamil as an internal standard. After centrifugation at 2,451 g for 10 min at 4 °C, samples were filtered and further diluted 5-fold with water containing internal standard, aliquots of which were analyzed by LC-MS/MS to determine plasma concentrations of BI-639667.

Bioanalysis of plasma

For quantitation of BI-639667 in plasma, a 1290 Infinity II LC system (Agilent) connected to a Sciex 5500 QTRAP+ mass spectrometer (Sciex, Thornhill, ON, Canada) was used. Samples were separated on a Waters Acuity UPLC BEH C18 column (2.1 x 50 mm) (Waters), with a 1.7- μ m particle size. Mobile phase A consisted of water containing 0.1% formic acid (FA), and mobile phase B consisted of acetonitrile containing 0.1% FA. A 2.5-min UPLC mobile phase gradient was used at a flow rate of 0.4 mL/min with the following parameters: 5% B from 0 – 0.7 min, linear increase to 95% B from 0.7 – 1.0 min, hold at 95% B from 1.0 – 1.2 min, linear decrease to 5% B from 1.2 – 2.0 min, hold at 5% B from 2.0 – 2.5 min. A multiple reaction monitoring analysis was performed in the positive ionization mode for detection of BI-

639667 (mass to charge ratio (m/z) 452.1 \rightarrow 240) and verapamil (m/z) 458.29 \rightarrow 165.1). Concentrations of BI 639667 in plasma were determined using linear calibration standard curves with $1/x^2$ weighting using Analyst® software, version 1.7 (Sciex, Thornhill, ON, Canada). The lower limit of quantitation (LLOQ) for BI-639667 in plasma samples was 19.5 nmol/L.

Pharmacokinetic analysis

Exposure values (C_{max} and AUC_{0-48}) were calculated for each individual plasma concentration-time profile by non-compartmental methods using the software, ToxKin (Entimo, Germany). Plasma samples where concentrations of BI-639667 were below the limit of quantitation (BLQ) were set to 0 nmol/L for PK analysis. Dose-normalized exposure values were then calculated using the potency factor for each form of BI-639667. The relative oral bioavailability for each BI-639667 solid form, compared to the BI-639667 solution, was calculated by dividing the dose-normalized AUC_{0-48} value for each form by the AUC_{0-48} value for BI-639667 in solution.

Results and Discussion

Validation of the ASD apparatus

The performance of the artificial stomach and duodenum (ASD) apparatus using in this study was first validated by comparing the experimentally measured concentration - time profiles with the theoretically predicted profiles in both chambers using a solution of acetaminophen (Figure 2).

The mass-balance equations in the gastric and duodenal chambers are given in equations (1) and (2), respectively:

$$\frac{d(C_s V_s)}{dt} = -RC_s \tag{1}$$

$$\frac{V_d dC_d}{dt} = C_s R - C_d (b + R) \tag{2}$$

In the equations, C represents concentration of drug, V represents fluid volume, and subscripts "s" and "d" denote stomach chamber and duodenum chamber, respectively. The parameter b(mL/min) is secretion rate of fresh duodenal fluid, and R (mL/min) is stomach emptying rate, which is given by equation (3):

$$R = a + k(V_s - V_r) \tag{3}$$

Where a (mL/min) is the secretion rate of fresh gastric fluid into stomach chamber; k (min^{-1}) is emptying constant, V_s (mL) is the total volume of liquid in stomach chamber at any time point and V_r (mL) is the resting volume in stomach chamber.

In this study, a solution of acetaminophen, a weak acid with a p K_a of 9.5, was selected due to its high aqueous solubility (approximately 20.3 mg/mL at 37 °C) (Prescott, 1980; Shaw et al., 2005), which eliminates the possibility of precipitation during the ASD experiments. An absence of any precipitation in both chambers was also visually confirmed throughout the experiments. The measured and predicted concentration – time profiles in both chambers were in excellent agreement (Figure 2). This result confirms that the ASD apparatus was working properly.

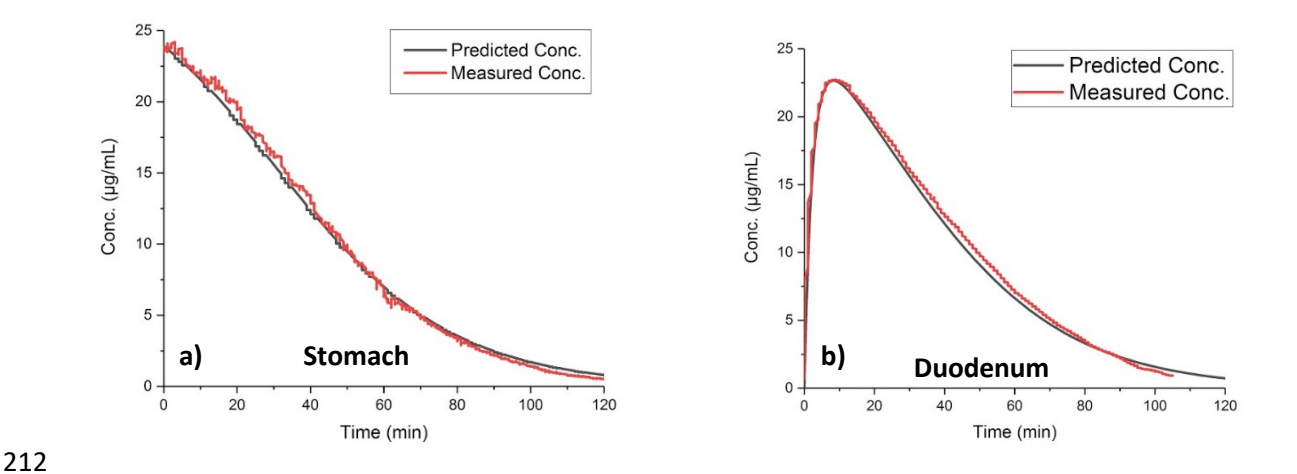


Figure 2. Experimental and theoretical concentration – time profiles of an acetaminophen solution in a) stomach chamber and b) duodenum chamber of the ASD apparatus.

Characterization of BI-639667 solid forms

The phase identification and purity of prepared solid forms of BI-639667 were verified by a good match between experimental and theoretical PXRD patterns (calculated from corresponding single crystal structures) of each form (Figure 3). Although the experimental PXRD pattern of the maleate salt closely resembles the PXRD calculated from crystal structure, peaks in the >15° 2-theta angles region of the experimental PXRD pattern shifted to lower positions. This is attributed to the crystal lattice expansion since the experimental data was collected at a temperature (~298 K) significantly higher than the temperature (100 K) at which the crystal structure was solved. We note that, although crystal structures of these solid forms were solved by us, they are not discussed here as the current work focuses on the predictive performance of *in vitro* ASD dissolution. Detailed discussion of the single crystal structures of different solid forms will be given in a future publication.

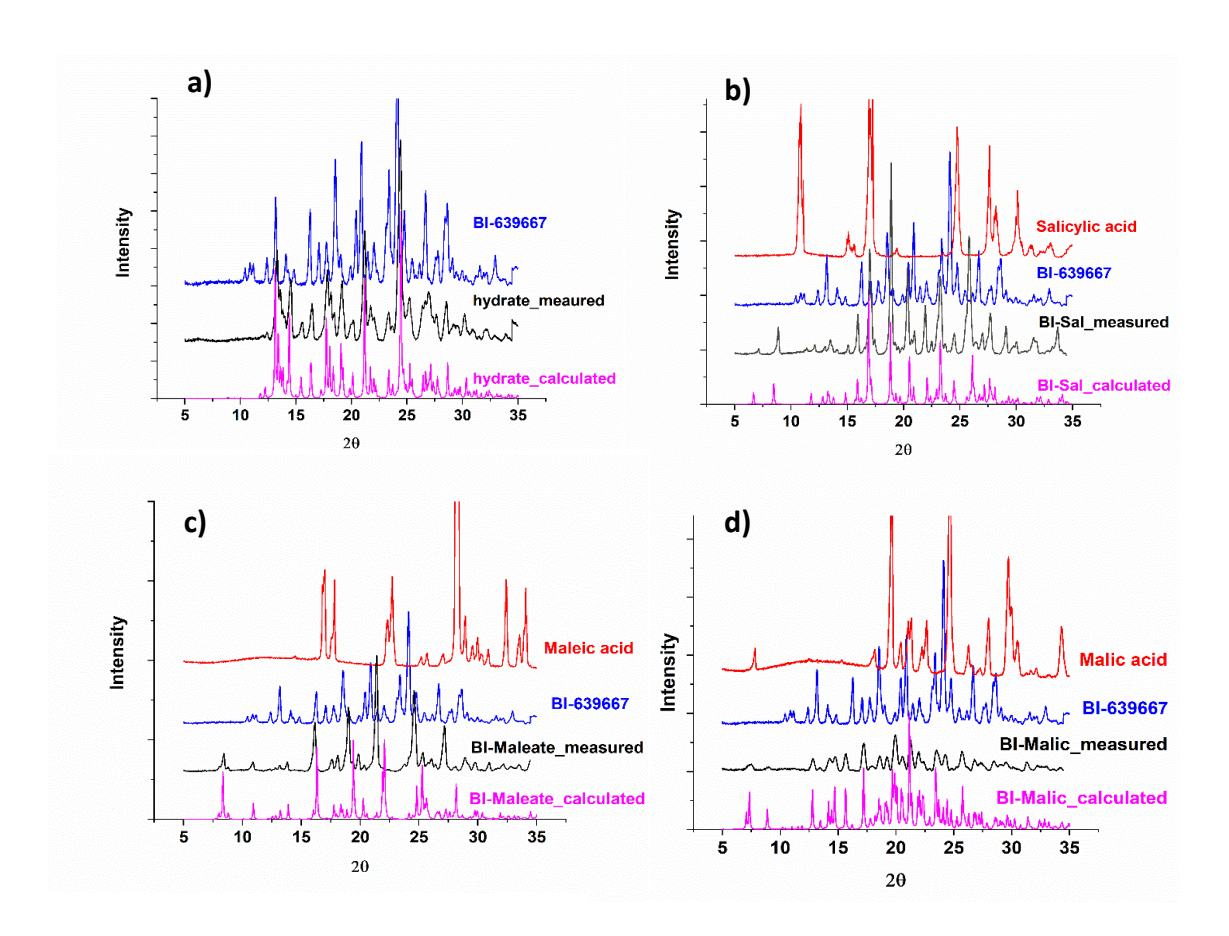


Figure 3. PXRD patterns of BI-639667 solid forms, a) monohydrate, b) salicylic acid cocrystal, c) maleate salt, d) malate salt.

In vitro dissolution in artificial stomach and duodenum (ASD)

In this study, an equivalent dose of 30 mg BI-639667 was used in all the formulations. For the BI-639667 solution formulation, the measured concentration - time profile reasonably matches with the predicted profile (Figure 4a), indicating an absence of precipitation during the experiment (Polster et al., 2015), despite the reduced solubility of BI-639667 in duodenum (pH 6.4) compare to that in stomach (pH 2) (Table S1 and Figure S2). This is consistent with the validation study using acetaminophen. Hence, its AUC would correspond to the maximum exposure of BI-639667 when a 30 mg dose was used in this study. The dissolution profiles of the four BI-639667 solid forms in the duodenum chamber varied significantly (Figure 4b), where the AUC follows the descending order of solution > salicylic acid cocrystal > maleate salt > malate salt > monohydrate. This rank order is the same as that in the stomach chamber (Figure S4).

Table 1. Pharmacokinetic parameters of different formulations of BI-639667 based on the concentration - time profiles in the ASD duodenum chamber (mean \pm SD, n = 3)

	Solution	Salicylic Acid Cocrystal	Maleate Salt	Malate salt	Monohydrate
AUC (μg/mL*min), 0-90 min	3664 ± 178	1664 ± 75	693 ± 48	529 ± 74	234 ± 10
Relative AUC (%)	100	45.4	19.0	14.4	6.4
C_{\max} (mL/min)	85.95 ± 0.47	24.39 ± 0.85	9.86 ± 0.66	7.62 ± 0.94	3.45 ± 0.13

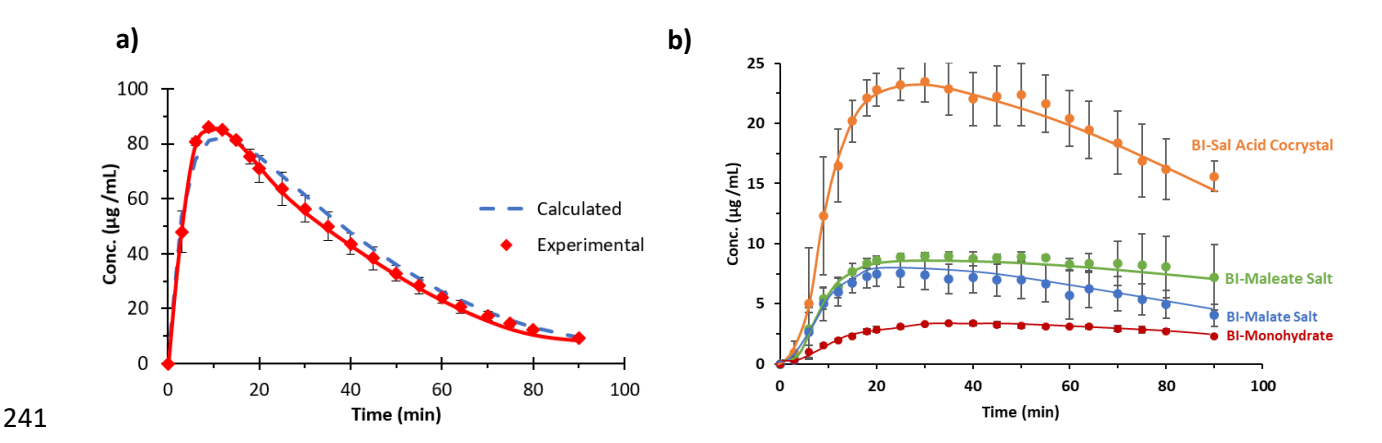


Figure 4. Duodenum concentration - time profiles obtained from the *in vitro* ASD experiments for different formulations of BI-639667, a) solution, and b) four solid forms (n = 3).

For different solid forms of a given API, solubility is a driving force for dissolution rate (Noyes and Whitney, 1897), where a higher solubility favors faster dissolution. This explains the much greater AUC of the *in vitro* dissolution profile of the salicylic acid cocrystal, which is more soluble (92.19 \pm 1.62 µg/mL in water at room temperature) than the monohydrate form (solubility = 5.43 ± 0.21 µg/mL in water at room temperature). For the salicylic acid cocrystal, K_{sp} is the square of its solubility based on its 1:1 stoichiometry. Importantly, salicylic acid cocrystal also showed highest phase stability during the course of both IDR (>15 min in pH 1.2 HCl medium, Figure S3) and polymer stabilization studies based on PXRD data (Table S2). Thus, its solubility advantage over the monohydrate was realized during the ASD experiment, consequently resulting in the highest duodenum AUC (1664 ± 75 µg/mL*min). In contrast, maleate salt converted to an anhydrate and malate salt converted to the monohydrate when exposed to the pH 1.2 HCl medium even in the presence of polymers (Figure S3 and Table S2), leading to only mildly increased duodenum AUC (693 ± 48 µg/mL*min for maleate salt and 529 ± 74 µg/mL*min for malate salt) than the monohydrate (234 ± 10 µg/mL*min). Such phase conversion more likely occurred within the diffusion layer of solid particles when exposed to the gastric medium so that the surface of particles were covered by a layer of the less soluble solid form, resulting in reduced dissolution rate (Hawley and

Morozowich, 2010). Since the hydrate usually is less soluble than the anhydrate (Bhatia et al., 2018), duodenum AUC of the maleate salt was higher than the malate salt (Table 1 and Figure 4).

Bioavailability in rats

Based on the plasma concentration-time profiles of the five formulations in rats (Figure 5), pharmacokinetic parameters were obtained (Table 2). The AUC values of BI-639667 in plasma decrease based on the formulation of BI-639667 administered in the following order: solution > salicylic acid cocrystal > maleate salt > malate salt > hydrate, which is identical to the trend observed in the ASD study. The plasma exposure was the highest following oral administration of BI-639667 in solution and was the lowest following administration of the monohydrate. Among the four solid forms, the salicylic acid cocrystal exhibited the highest relative oral bioavailability of 74% compared to the solution. Meanwhile, the more soluble maleate salt and malate salt solid forms exhibited significantly lower AUC than the salicylic acid cocrystal, again likely due to precipitation of the monohydrate during the experiment. Consequently, only slight improvement of AUC was observed following administration of these forms compared to the poorly soluble monohydrate form.

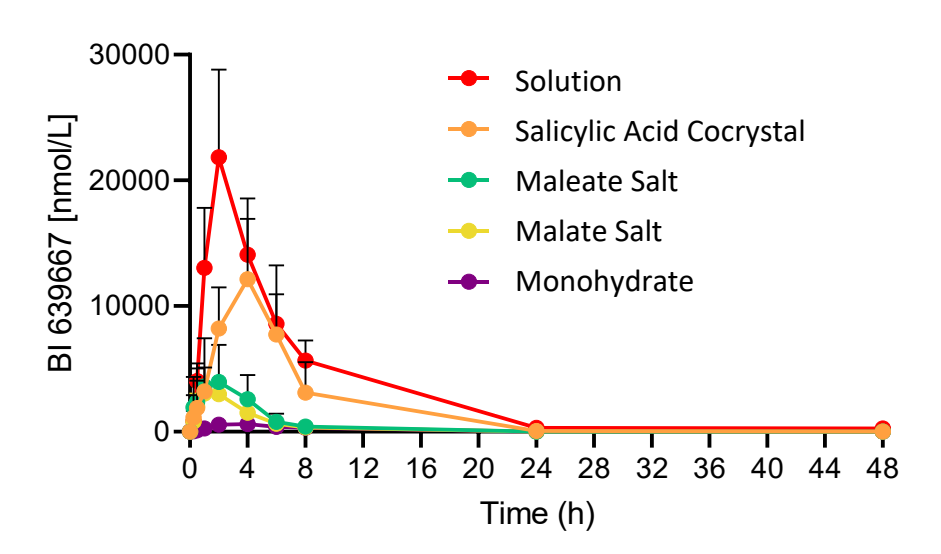


Figure 5. Mean plasma concentration-time profiles of BI-639667 in rats following single oral administration of 50 mg/kg BI-639667 as different formulations.

Table 2. Dose-normalized plasma exposure (C_{max} and AUC₀₋₄₈) of BI-639667 in rats (n = 4), following oral administration of five different formulations. Values represent mean \pm SD.

PK parameter	Solution	Salicylic Acid Cocrystal	Maleate Salt	Malate Salt	Monohydrate	
$C_{ m max}/{ m dose},$	437 ±	355 ±	107 ±	80.0 ±	14.0 ± 5.34	
(nmol/L)/(mg/kg)	140	130	85.7	19.7	14.0 ± 3.34	
AUC ₀₋₄₈ /dose,	2,990 ±	2,210 ±	520 ±	400 ±	127 ± 53.0	
$(nmol \cdot h/L)/(mg/kg)$	729	1,050	411	82.6		
Relative oral bioavailability (%)	100	73.9	17.4	13.4	4.24	

Both the AUC and C_{max} from the *in vitro* ASD study correlate strongly with those from the *in vivo* pharmacokinetic study (Figure 6). Thus, ASD reasonably predicted the *in vivo* relative bioavailability in rats. In comparison to the animal studies, results from the ASD study are significantly more precise than that of the *in vivo* results, demonstrating ASD could serve as a useful *in vitro* tool for facilitating solid form selection and formulation development of drugs by providing knowledge of potential *in vivo* behaviors early. We caution that *in vivo* bioavailability can vary from species to species. Thus, although the results from this study are exciting, it remains to be confirmed that such predictions can be reliably extrapolated to humans. For practically reasons, the volumes of gastric and duodenal fluids used in the ASD experiments were significantly larger than physiological volumes in rats. This likely has an influence on absolute dissolution profiles, but we did not expect the rank-order of different formulations to be significantly affected. Moreover, we used simple dissolution media instead of bio-relevant media containing surfactant and lipids in the ASD experiments. This is expected to affect absolute concentration – time profiles but we assumed that its impact on the rank order of these formulations is low. The gastric pH 1.2 in the ASD experiments is lower than the average gastric pH in rats (pH ~4) (McConnell et al., 2010). This can

potentially impact the degree of supersaturation and, hence, precipitation kinetics during ASD experiments. Those should be further examined in future studies based on ASD. Also, the use of TPGS in the solution formulation may enhance permeability of this compound, which is an effect not present in the rats PK studies of other formulations. This effect, if present, is only expected to slightly shift the plasma concentration – time profile of the solution formulation in rats because of the high permeability of this compound. In any case, the rank order should not be affected by this.

For this model API, the knowledge of solubility and phase stability of different solid forms could be used to predict the highest relative bioavailability of the salicylic acid cocrystal and lowest relative bioavailability of the monohydrate. However, there is no enough information for predicting the relative bioavailability of the two salts that underwent fast phase change during the dissolution experiments. Additionally, solubility is an equilibrium properties, which is not affected by particle size. Consequently, it won't be able to account for the effect by different particle size and surface area. Thus, the ASD approach provides more reliable predictions than those based on solubility alone. Finally, for APIs with high permeability, fast absorption of API can affect the degree of supersaturation. This is not predicted by the current ASD setup, which does not consider absorption. More accurate predictions would be obtained if the absorption process can be incorporated in an improved ASD apparatus. However, this new functionality should be pursued only if it does not come with a significant barrier for routine use in a preclinical setting.

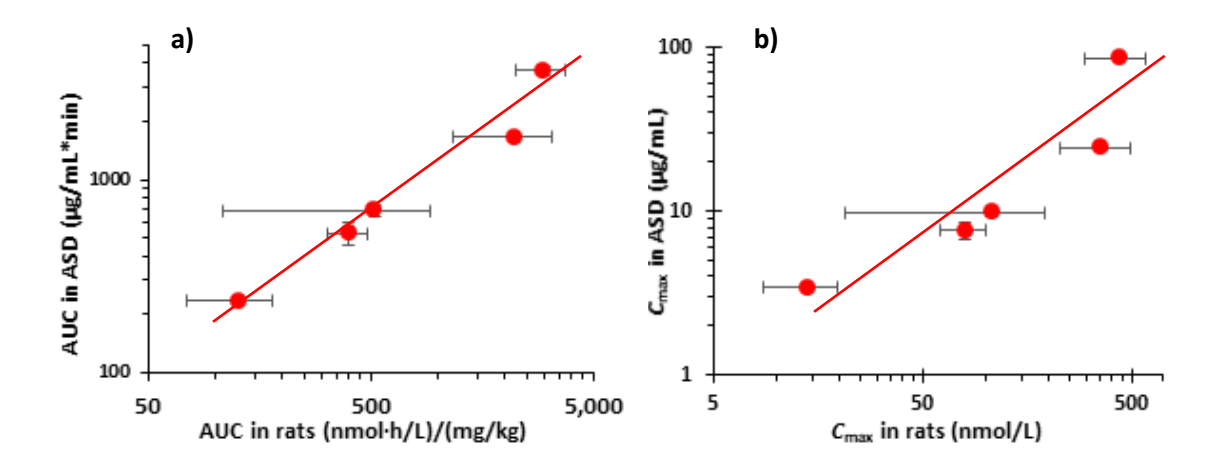


Figure 6. Comparison of predicted pharmacokinetic parameters from ASD study and *in vivo* study, a) AUC and b) C_{max} . The points are, in ascending order, monohydrate, malate salt, maleate salt, salicylic acid cocrystal, and solution.

Conclusion

Using BI-639667, a BCS II compound, we have shown that the *in vitro* ASD apparatus successfully predicted the rank order of relative bioavailability of its different solid forms. In this example, the solid form capable of maintaining supersaturation the longest (the salicylic acid cocrystal) exhibits the greatest AUC and C_{max} in both the ASD experiment and the rat study. This, along with other published examples, suggests that ASD is an effective tool for understanding dissolution behaviors of different solid forms and/or formulations of BCS II compounds, particularly formulations that induce and maintain supersaturation. When properly integrated in the workflow, the ASD can potentially be used to guide solid form selection and formulation optimization of such compounds in a material sparing and expedited manner.

Acknowledgement

CCS thanks the National Science Foundation for support through the Industry University

Collaborative Research Center (IUCRC) grant IIP-2137264, Center for Integrated Materials Science and

Engineering for Pharmaceutical Products (CIMSEPP). Assistance from Ms. Xueyao Hu in the crystal

phase stability experiments and ASD data collection is acknowledged.

Data in this paper is available upon request.

References

Bhatia, A., Chopra, S., Nagpal, K., Deb, P.K., Tekade, M., Tekade, R.K., 2018. Chapter 2 - Polymorphism and its Implications in Pharmaceutical Product Development, in: Tekade, R.K. (Ed.), Dosage Form Design Parameters. Academic Press, pp. 31-65.

Carino, S.R., Sperry, D.C., Hawley, M., 2006. Relative bioavailability estimation of carbamazepine crystal forms using an artificial stomach-duodenum model. Journal of pharmaceutical sciences 95, 116-125.

Carino, S.R., Sperry, D.C., Hawley, M., 2010. Relative bioavailability of three different solid forms of PNU-141659 as determined with the artificial stomach-duodenum model. Journal of pharmaceutical sciences 99, 3923-3930.

Chen, D., Huang, W., Zhang, Q., Zhang, Z., Guo, Y., Vreeman, G., Sun, C.C., Hawley, M., Yang, B.-S., He, X., 2022. Bioavailability-Enhancing Cocrystals: Screening, In Vivo Predictive Dissolution, and Supersaturation Maintenance. Crystal Growth & Design 22, 5154-5167.

Dressman, J.B., 1986. Comparison of canine and human gastrointestinal physiology. Pharmaceutical Research 3, 123-131.

Fotaki, N., Vertzoni, M., 2010. Biorelevant dissolution methods and their applications in in vitro-in vivo correlations for oral formulations. The Open Drug Delivery Journal 4.

Guo, Y., Sun, C.C., 2022. Profound effects of gastric secretion rate variations on the precipitation of erlotinib in duodenum – An in vitro investigation. International Journal of Pharmaceutics 619, 121722.

Hawley, M., Morozowich, W., 2010. Modifying the diffusion layer of soluble salts of poorly soluble basic drugs to improve dissolution performance. Mol Pharm 7, 1441-1449.

Kararli, T.T., 1995. Comparison of the gastrointestinal anatomy, physiology, and biochemistry of humans and commonly used laboratory animals. Biopharmaceutics & drug disposition 16, 351-380.

Kaur, N., Thakur, P.S., Shete, G., Gangwal, R., Sangamwar, A.T., Bansal, A.K., 2020. Understanding the oral absorption of irbesartan using biorelevant dissolution testing and PBPK modeling. AAPS PharmSciTech 21, 1-13.

Kostewicz, E.S., Wunderlich, M., Brauns, U., Becker, R., Bock, T., Dressman, J.B., 2004. Predicting the precipitation of poorly soluble weak bases upon entry in the small intestine. The Journal of pharmacy and pharmacology 56, 43-51.

Lee, C.-M., Luner, P.E., Locke, K., Briggs, K., 2017. Application of an Artificial Stomach-Duodenum Reduced Gastric pH Dog Model for Formulation Principle Assessment and Mechanistic Performance Understanding. Journal of pharmaceutical sciences 106, 1987-1997.

McConnell, E.L., Basit, A.W., Murdan, S., 2010. Measurements of rat and mouse gastrointestinal pH, fluid and lymphoid tissue, and implications for in-vivo experiments. Journal of Pharmacy and Pharmacology 60, 63-70.

Mithani, S.D., 1998. Dissolution and precipitation of dipyridamole: Effect ofpH and bile salt concentration. University of Michigan.

Mudie, D.M., Murray, K., Hoad, C.L., Pritchard, S.E., Garnett, M.C., Amidon, G.L., Gowland, P.A., Spiller, R.C., Amidon, G.E., Marciani, L., 2014. Quantification of Gastrointestinal Liquid Volumes and Distribution Following a 240 mL Dose of Water in the Fasted State. Molecular Pharmaceutics 11, 3039-3047.

Mudie, D.M., Samiei, N., Marshall, D.J., Amidon, G.E., Bergström, C.A.S., 2020. Selection of In Vivo Predictive Dissolution Media Using Drug Substance and Physiological Properties. The AAPS Journal 22, 34. Noyes, A.A., Whitney, W.R., 1897. THE RATE OF SOLUTION OF SOLID SUBSTANCES IN THEIR OWN SOLUTIONS. Journal of the American Chemical Society 19, 930-934.

P. Heinrich Stahl, C.G.W., International Union of Pure and Applied Chemistry, 2002. Handbook of pharmaceutical salts: properties, selection, and use.

Polster, C.S., Atassi, F., Wu, S.-J., Sperry, D.C., 2010. Use of Artificial Stomach–Duodenum Model for Investigation of Dosing Fluid Effect on Clinical Trial Variability. Molecular Pharmaceutics 7, 1533-1538.

Polster, C.S., Wu, S.-J., Gueorguieva, I., Sperry, D.C., 2015. Mechanism for Enhanced Absorption of a Solid Dispersion Formulation of LY2300559 Using the Artificial Stomach Duodenum Model. Molecular Pharmaceutics 12, 1131-1140.

Prescott, L.F., 1980. Kinetics and metabolism of paracetamol and phenacetin. British journal of clinical pharmacology 10 Suppl 2, 291s-298s.

Shah, B., Dong, X., 2022. Design and Evaluation of Two-Step Biorelevant Dissolution Methods for Docetaxel Oral Formulations. AAPS PharmSciTech 23, 113.

Shaw, L.R., Irwin, W.J., Grattan, T.J., Conway, B.R., 2005. The effect of selected water-soluble excipients on the dissolution of paracetamol and ibuprofen. Drug development and industrial pharmacy 31, 515-525. Takeuchi, S., Tsume, Y., Amidon, G.E., Amidon, G.L., 2014. Evaluation of a three compartment in vitro gastrointestinal simulator dissolution apparatus to predict in vivo dissolution. Journal of pharmaceutical sciences 103, 3416-3422.

Tsume, Y., Ashworth, L., Bermejo, M., Cheng, J., Cicale, V., Dressman, J., Fushimi, M., Gonzalez-Alvarez, I., Guo, Y., Jankovsky, C., Lu, X., Matsui, K., Patel, S., Sanderson, N., Sun, C.C., Thakral, N.K., Yamane, M., Zöller, L., 2023. Harmonizing Biopredictive Methodologies Through the Product Quality Research Institute (PQRI) Part I: Biopredictive Dissolution of Ibuprofen and Dipyridamole Tablets. The AAPS Journal 25, 45. Tsume, Y., Takeuchi, S., Matsui, K., Amidon, G.E., Amidon, G.L., 2015. In vitro dissolution methodology, mini-Gastrointestinal Simulator (mGIS), predicts better in vivo dissolution of a weak base drug, dasatinib. European journal of pharmaceutical sciences: official journal of the European Federation for Pharmaceutical Sciences 76, 203-212.

Vrbanac, H., Trontelj, J., Berglez, S., Petek, B., Opara, J., Jereb, R., Krajcar, D., Legen, I., 2020. The biorelevant simulation of gastric emptying and its impact on model drug dissolution and absorption kinetics. European Journal of Pharmaceutics and Biopharmaceutics 149, 113-120.

Wang, C., Chopade, S.A., Guo, Y., Early, J.T., Tang, B., Wang, E., Hillmyer, M.A., Lodge, T.P., Sun, C.C., 2018. Preparation, Characterization, and Formulation Development of Drug–Drug Protic Ionic Liquids of Diphenhydramine with Ibuprofen and Naproxen. Molecular Pharmaceutics 15, 4190-4201.

Wang, Q., Fotaki, N., Mao, Y., 2009. Biorelevant dissolution: Methodology and application in drug development. Dissolution Technologies 16, 6-12.

Zhou, Z., Dunn, C., Khadra, I., Wilson, C.G., Halbert, G.W., 2017. Statistical investigation of simulated fed intestinal media composition on the equilibrium solubility of oral drugs. European journal of pharmaceutical sciences: official journal of the European Federation for Pharmaceutical Sciences 99, 95-104.

Zoeller, T., Klein, S., 2007. Simplified biorelevant media for screening dissolution performance of poorly soluble drugs. Dissolution Technol 14, 8-13.